© 2015. Published by The Company of Biologists Ltd | Journal of Cell Science (2015) 128, 3502-3513 doi:10.1242/jcs.174409

RESEARCH ARTICLE

The caspase-3–p120-RasGAP module generates a NF-κB repressor in response to cellular stress

Hadi Khalil[1,*], Noureddine Loukili[1,*], Alexandre Regamey[2], Alvaro Cuesta-Marban[1], Elettra Santori[1], Marcel Huber[2] and Christian Widmann[1,‡]

ABSTRACT

The nuclear factor κB (NF-κB) transcription factor is a master regulator of inflammation. Short-term NF-κB activation is generally beneficial. However, sustained NF-κB might be detrimental, directly causing apoptosis of cells or leading to a persistent damaging inflammatory response. NF-κB activity in stressed cells needs therefore to be controlled for homeostasis maintenance. In mildly stressed cells, caspase-3 cleaves p120 RasGAP, also known as RASA1, into an N-terminal fragment, which we call fragment N. We show here that this fragment is a potent NF-κB inhibitor. Fragment N decreases the transcriptional activity of NF-κB by promoting its export from the nucleus. Cells unable to generate fragment N displayed increased NF-κB activation upon stress. Knock-in mice expressing an uncleavable p120 RasGAP mutant showed exaggerated NF-κB activation when their epidermis was treated with anthralin, a drug used for the treatment of psoriasis. Our study provides biochemical and genetic evidence of the importance of the caspase-3–p120-RasGAP stress-sensing module in the control of stress-induced NF-κB activation.

KEY WORDS: Caspase, Cellular stress, NF-κB, RasGAP

INTRODUCTION

Nuclear factor κB (NF-κB) was discovered and characterized as a transcription factor that binds to a site in the promoter of the immunoglobulin κ chain and that is required for B-lymphocyte-specific gene expression (Sen and Baltimore, 1986b). However, subsequent studies have shown that NF-κB can be activated in various cell types (Sen and Baltimore, 1986a). NF-κB is ubiquitously expressed and serves as a crucial regulator for the expression of many genes (Baldwin, 1996). The NF-κB family in mammalian cells comprises five members: p65 (also known as RelA), RelB, c-Rel, NF-κB1 (p50 and p105) and NF-κB2 (p52 and p100). RelA, RelB and c-Rel, are synthesized as transcriptionally active proteins, whereas NF-κB1 and NF-κB2 are synthesized as longer precursor molecules of 105 and 100 kDa, respectively, that are then processed by proteolytic cleavage into the smaller, transcriptionally active, p50 and p52 forms (reviewed extensively by Baldwin, 1996; Barnes, 1997; Verma et al., 1995; May and Ghosh, 1998; Kopp and Ghosh, 1995; Vallabhapurapu and Karin, 2009). NF-κB homo- or hetero-dimers are sequestered in the cytosol of unstimulated cells through non-covalent interactions with a class of inhibitory proteins called inhibitors of κB (IκBs) (Baldwin, 1996; Li and Verma, 2002; May and Ghosh, 1998). Signals that induce NF-κB activation through the so-called canonical (or classical) pathway trigger the activation of the upstream IκB kinase complex (IKK), containing the IKKα and IKKβ catalytic subunits and the IKKγ (also called Nemo) regulatory subunit. This complex then phosphorylates IκB proteins, leading to their degradation. Thus, NF-κB is no longer sequestered in the cytoplasm and is then free to translocate to the nucleus where it can regulate expression of genes containing NF-κB-binding elements (Bonizzi and Karin, 2004; Oeckinghaus et al., 2011). In the non-canonical (or alternative) NF-κB activation pathway, NF-κB2 (p100) binds and sequesters RelB in the cytoplasm. In the presence of an appropriate stimulus [e.g. CD40 or BAFF receptor (also known as TNFRSF13C) stimulation], IKKα is activated by the NF-κB inducing kinase (NIK, also known as MAP3K14) and this in turn leads to partial degradation of p100 into the p52 NF-κB subunit. The latter, still associated with RelB, can then translocate to the nucleus and regulate gene transcription (Gardam and Brink, 2014; Vallabhapurapu and Karin, 2009).

NF-κB exerts complex regulatory functions in the control of inflammation. It can either promote or inhibit inflammation depending on the tissues, the activation stimulus and the stage of the inflammation process (Lawrence, 2009; Lawrence and Fong, 2010). In the skin, disruption of the NF-κB activation pathway, for example by overexpressing a degradation-resistant IkBα mutant (Stratis et al., 2006) or by genetic removal of IKKβ (Pasparakis et al., 2002), induces a severe and often lethal inflammatory response (reviewed in Laychock et al., 2006). In this case, therefore, NF-κB exerts anti-inflammatory functions. By contrast, NF-κB activation is crucially required for the release of pro-inflammatory cytokines from tissues exposed to pathogen-associated molecular patterns and damage-associated molecular patterns (Baker et al., 2011; Newton and Dixit, 2012; Vallabhapurapu and Karin, 2009) and activation of immune cells recruited to the inflammation site (Gerondakis et al., 2014; Vallabhapurapu and Karin, 2009). Hence, NF-κB plays a complex role in inflammation because it can initiate inflammation, but it is also involved in its resolution (Lawrence and Fong, 2010).

There is evidence that NF-κB activity can be modulated by some members of the caspase family of proteases in non-apoptotic cells (Lamkanfi et al., 2007). In *Drosophila*, DREDD, the ortholog of caspase-8 (an upstream caspase), is required for the activation of the NF-κB ortholog Relish (Stoven et al., 2003). In mammals, T cell receptor stimulation leads to NF-κB activation. Although not indispensable (Salmena et al., 2003), caspase-8 favors and accelerates this response (Su et al., 2005). The capacity of caspase-8 to modulate NF-κB is seemingly structural as it also occurs in cells expressing a catalytically inactive caspase-8 (Chaudhary et al., 2000; Lamkanfi et al., 2005) or when caspase activity is inhibited (Kreuz et al., 2004).

[1]Department of Physiology, Biology and Medicine Faculty, University of Lausanne, 1005 Lausanne, Switzerland. [2]Department of Dermatology, Lausanne University Hospital, 1011 Lausanne, Switzerland.
*These authors contributed equally to this work

‡Author for correspondence (Christian.Widmann@unil.ch)

Received 15 May 2015; Accepted 27 July 2015

Journal of Cell Science (2015) 128, 3502-3513 doi:10.1242/jcs.174409

p120 RasGAP (also known as RASA1, hereafter RasGAP), is an unconventional caspase substrate because, depending on the extent of its cleavage by caspase-3, it induces either an anti-apoptotic response or favors cell death (Khalil et al., 2014; Yang et al., 2005b; Yang and Widmann, 2001). At low levels of caspase-3 activity, RasGAP is cleaved at position 455, generating an N-terminal fragment (fragment N) that induces the anti-apopototic Akt pathway (Yang et al., 2004; Yang and Widmann, 2001, 2002). At higher levels of caspase-3 activity, fragment N is further cleaved at position 157 shutting off its capacity to stimulate Akt (Yang et al., 2005b). Several downstream targets of Akt are activated or repressed by direct or indirect phosphorylation. Akt can mediate NF-κB activation by directly phosphorylating IKKα at threonine 23 (Ozes et al., 1999) or indirectly through cancer osaka thyroid (Cot, also known as MAP3K8), a serine/threonine kinase of the mitogen-activated protein kinase kinase kinase (MAP3K) family (Kane et al., 2002). However, despite the fact that fragment N activates Akt, its ability to protect cells does not depend on NF-κB (Yang and Widmann, 2002).

Here, we show that fragment N is a general NF-κB repressor in stressed cells. This inhibitory activity relies on the promotion of NF-κB nuclear export. Fragment N generation is required to control the extent of NF-κB activation in the skin in response to anthralin, a drug used to treat psoriasis. Cleavage of RasGAP by caspase-3 therefore represents a newly described mechanism used by cells and tissues to regulate NF-κB-dependent responses activated by stress.

RESULTS

Fragment N inhibits Akt-mediated NF-κB activity

The caspase-3-generated RasGAP-derived fragment N induces an anti-apoptotic response through the activation of the Ras–phosphoinositide 3-kinase (PI3K)–Akt pathway (Yang and Widmann, 2002). Even though fragment N simulates Akt, which has the ability to activate NF-κB (Ozes et al., 1999; Romashkova and Makarov, 1999), fragment N expression in cells does not lead to NF-κB stimulation (Yang and Widmann, 2002). This raises the possibility that fragment N inhibits Akt-induced NF-κB activity. To test this assumption, Akt was stimulated either by expression of the constitutively active V12 Ras mutant or through the expression of fragment N. This led to similar Akt stimulation as assessed by its phosphorylation on Ser473 and phosphorylation of GSK3β, one of its downstream targets (Cross et al., 1995) (Fig. 1A; quantification shown in Fig. 1B,C). Activation of Akt by fragment N is Ras-dependent as it was completely abolished by the overexpression of the dominant-negative N17 Ras mutant (supplementary material Fig. S1; Yang and Widmann, 2002). V12 Ras, as expected, stimulated NF-κB activity, but fragment N was able to completely block such activation (Fig. 1D). Given that the capacity of myristoylated (active) Akt (myr-Akt) to stimulate NF-κB was mild (Fig. 1E), we co-expressed the Cot kinase with myr-Akt, which has been shown to mediate strong Akt-induced NF-κB activation (Kane et al., 2002). The combination of myr-Akt and Cot indeed led to an even stronger NF-κB activation than V12 Ras; however, fragment N was still able to potently inhibit NF-κB activity (Fig. 1F). These results indicate that fragment N, although being

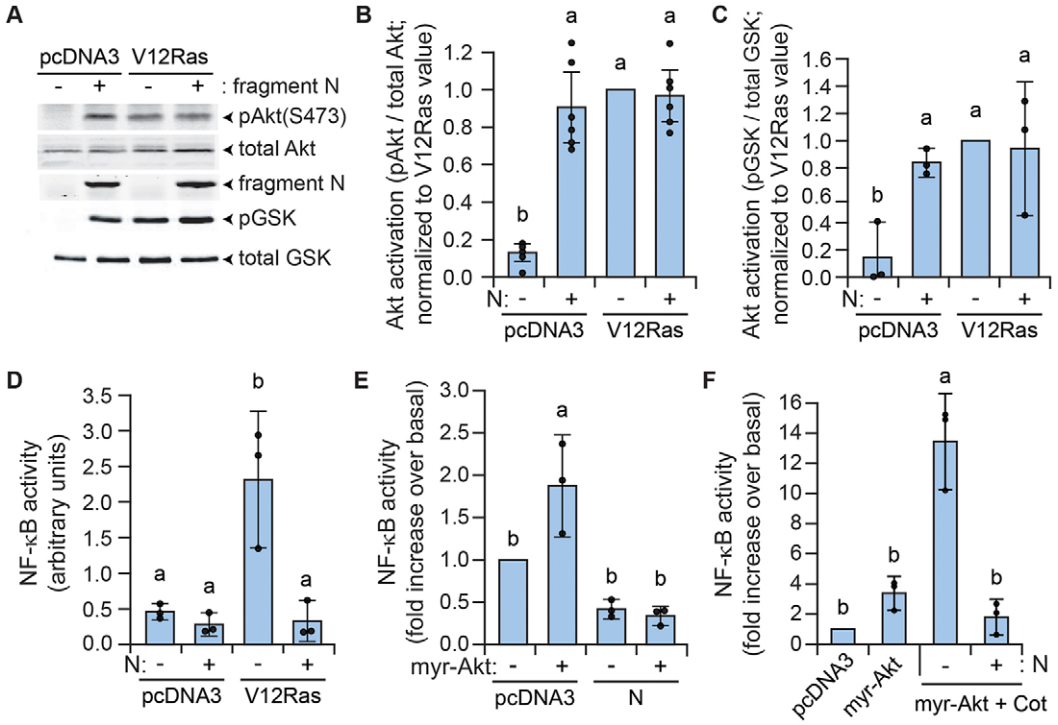

Fig. 1. Fragment N activates Akt in a Ras-dependent manner but hampers the ability of Akt to mediate NF-κB activation. (A–C) HeLa cells were co-transfected with an empty vector (pcDNA3) or with a V12Ras-encoding plasmid (V12Ras), with or without a fragment-N-encoding plasmid (N). Lysates were then analyzed by western blotting for the presence of the indicated proteins (panel A). Quantification of the phospho-Akt and phospho-GSK-3α/β is shown in panel B and C, respectively (three experiments performed in duplicate). (D–F) HeLa cells were transfected with 0.25 µg prLUC, an NF-κB reporter plasmid and 0.25 µg of pRL-TK *Renilla*-luciferase-encoding plasmid together with plasmids encoding the indicated constructs. NF-κB activity was measured by a luciferase assay and expressed as a fold increase over basal (D, three experiments performed in duplicate; E, eight individual experiments; F, three experiments performed in duplicate). Results are shown as mean±95% confidence intervals and are statistically different (P<0.05) when indicated with different lowercase letters.

Journal of Cell Science (2015) 128, 3502-3513 doi:10.1242/jcs.174409

able to activate Akt, prevents the latter from stimulating NF-κB-dependent transcription.

Fragment N inhibits NF-κB-dependent transcriptional activity in response to a variety of stimuli

To determine whether NF-κB inhibition mediated by fragment N is specific to Akt-dependent signals or whether it has a broader effect, we tested the ability of fragment N to inhibit NF-κB activity induced by a variety of stimuli that operate through either the canonical or non-canonical NF-κB pathways. The expression of fragment N in cells prevented NF-κB activity induced by the TNFα and IL-1β cytokines and by the lipopolysaccharide (LPS) bacterial toxin (Fig. 2A, upper row). The inhibition by fragment N of TNFα-stimulated NF-κB activity was confirmed by electromobility shift assay (EMSA) (Fig. 2B).

Ectopic expression of intracellular proteins that mediate NF-κB stimulation in response to ligand stimulation of cytokines and bacterial toxin receptors can lead to NF-κB activation. For example, expression of TRAF2 and TRAF6 in cells induces NF-κB stimulation through the canonical IKKα, IKKβ and IKKγ pathway (Chung et al., 2002). Overexpression of the ectodermal dysplasia receptor (EDAR) also leads to NF-κB activation through the canonical pathway (Kumar et al., 2001). Ectopic expression of NIK, by contrast, can induce NF-κB stimulation through the non-canonical IKKα pathway (Darding and Meier, 2012; Perkins, 2007). Fig. 2A (lower row) shows that, in each of these cases, fragment N expression in HeLa cells led to significant reduction in NF-κB activity.

We then monitored the nuclear accumulation of GFP-tagged p65 in different cell types stimulated with TNFα (Fig. 3A,B) or in conditions where NIK was overexpressed (Fig. 3C–E). This led to an increase in nuclear location of GFP–p65. However, when fragment N was present, TNFα- and NIK-induced p65 nuclear accumulation was significantly decreased. These data show that fragment N is a general NF-κB blocker that reduces the amount of NF-κB located in the nucleus.

To assess whether the domains carried by fragment N, when present in the context of the full-length RasGAP protein, would also be capable of inhibiting NF-κB, we overexpressed a caspase-3-resistant form of full-length RasGAP in cells. Supplementary material Fig. S2 shows that, in contrast to fragment N, full-length RasGAP was not able to significantly inhibit TNFα-induced NFκB activation. This supports the notion that RasGAP acquires its NF-κB

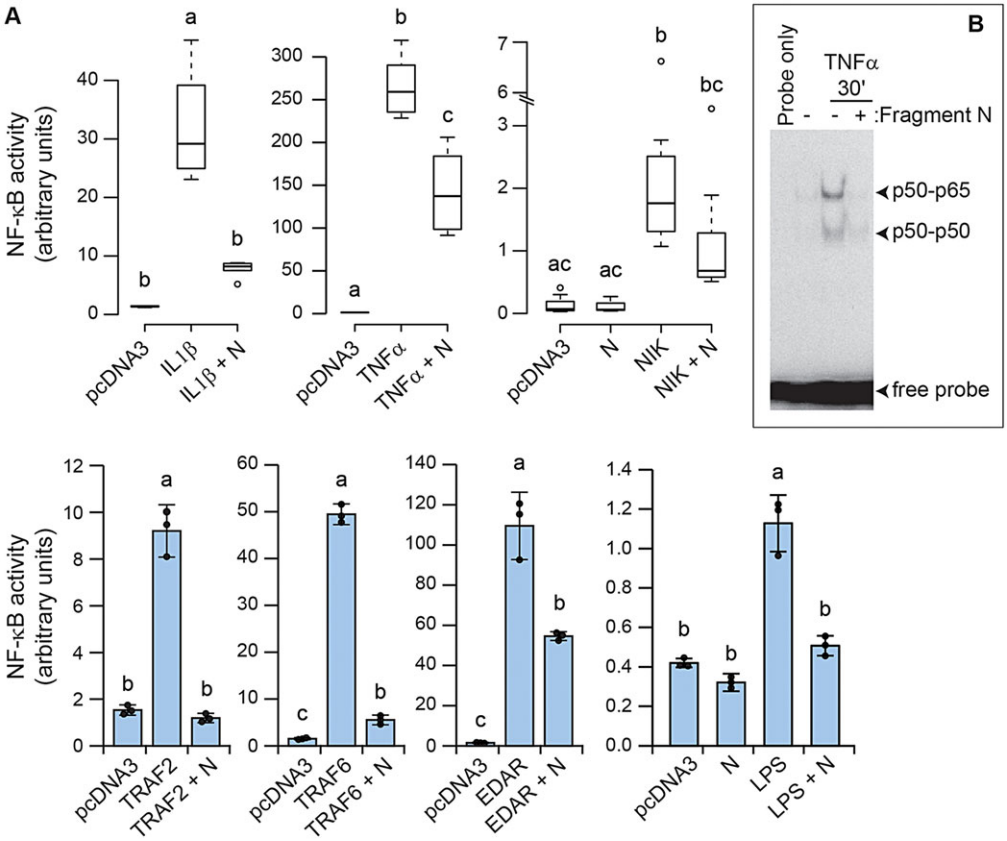

Fig. 2. Fragment N inhibits NF-κB activation in response to various stimuli. (A) HeLa cells were transfected with a combination of 0.25 µg prLUC, a firefly luciferase NF-κB reporter plasmid and 0.25 µg *Renilla*-luciferase-encoding pRL-TK plasmid in addition to empty plasmid (pcDNA3) or HA-tagged fragment N-encoding plasmid (N) as indicated. Cells were then stimulated with 1000 units/ml IL1β, 25 ng/ml human TNFα or 1 µg/ml LPS as indicated. Alternatively, HeLa cells were transfected with a combination of 0.25 µg prLUC and 0.25 µg of pRL-TK in addition to empty plasmid (pcDNA3), and plasmids encoding TRAF2, TRAF6, EDAR or NIK, in the presence or in the absence of HA-tagged fragment N-encoding plasmid (N) as indicated. NF-κB activity is expressed as the ratio of firefly to *Renilla* signal. When box-plots are displayed, center lines show the medians; box limits indicate the 25th and 75th percentiles as determined by the R software (http://www.r-project.org/); whisker lengths correspond to 1.5 times the box length (if shorter, the length of the whisker reaches the lowest or the highest value of the data set), outliers are represented by dots (n=6–7 sample points). In the lower panel, results are shown as mean±95% confidence intervals. Results are statistically different (P<0.05) when indicated with different lowercase letters. (B) HeLa cells were transfected or not with an HA-tagged fragment N-encoding plasmid; 24 h later, cells were treated or not with 25 ng/ml of human TNFα for 30 min. 5 µg of nuclear proteins were subjected to electrophoretic mobility shift assay (EMSA) using a DNA probe containing NF-κB-binding elements.

Journal of Cell Science (2015) 128, 3502-3513 doi:10.1242/jcs.174409

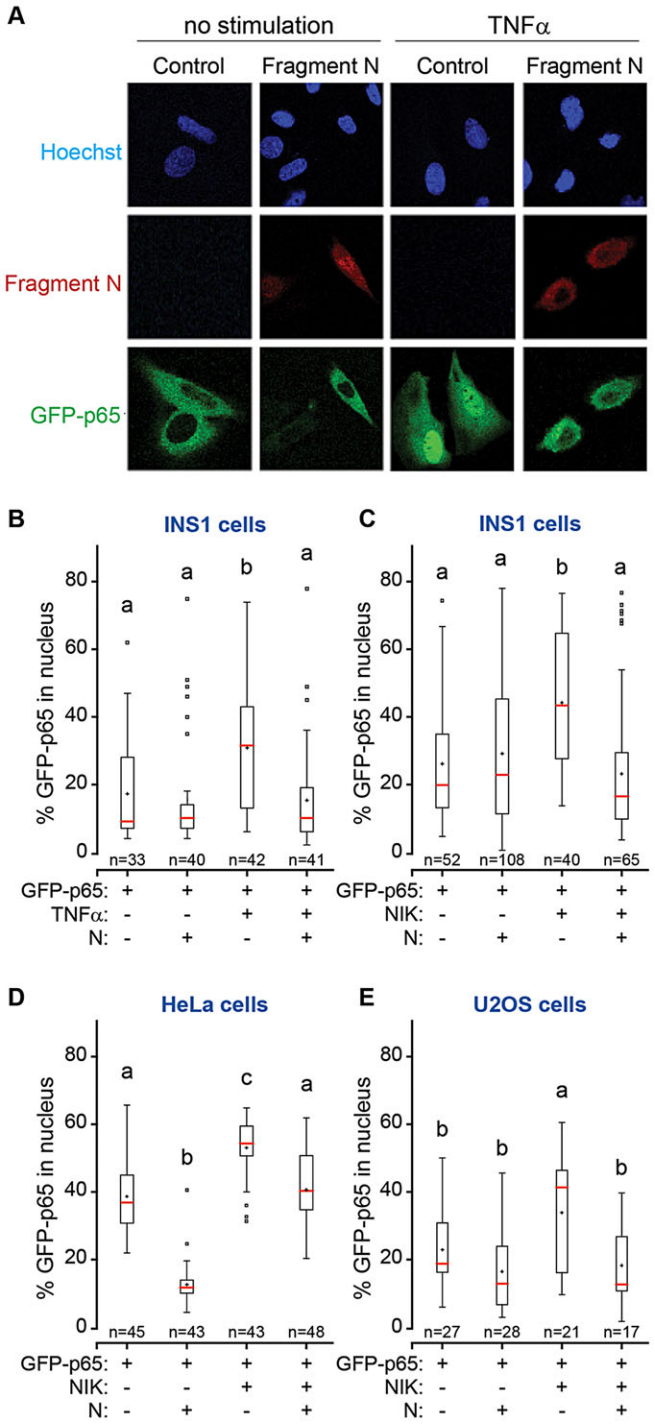

Fig. 3. Fragment N prevents p65 nuclear accumulation. (A) INS1 cells were plated on coverslips and transfected with a GFP–p65-encoding plasmid (GFP–p65), in the presence or absence of an HA-tagged fragment N-encoding plasmid (N). After 20 h, cells were stimulated for 30 min with 25 ng/ml TNFα. Then, cells were fixed and the nuclei were stained with Hoechst 33342. Immunocytochemistry was performed using an anti-HA antibody and the cells were photographed using a Zeiss confocal microscope. (B–E) INS1, HeLa, and U2OS cells were transfected with plasmids encoding the indicated constructs. In B, the cells were further stimulated or not for 30 min with 25 ng/ml human TNFα. The cells were then photographed as above and the percentage of GFP–p65 levels in the nucleus was determined as described in the Materials and Methods section. The cross in a box indicates the mean; the red line in a box indicates the median; box limits indicate the 25th and 75th percentiles as determined by the SAS 9.2 TS Level 2M0 software (SAS Institute Inc., Cary, NC); whisker lengths correspond to 1.5 times the box length (if shorter, the length of the whisker reaches the lowest or the highest value of the data set). Small squares represent outlier values. Results are statistically different (P<0.05) when indicated with different lowercase letters.

inhibitory function only when cleaved by caspase-3 (see also Figs 7 and 8).

Fragment N neither inhibits IκB degradation nor binds to NF-κB dimers

NF-κB dimers are sequestered in the cytoplasm through binding to IκB proteins (Ben-Neriah, 2002). Upon stimulation, the activated IKK complex phosphorylates IκBα. This targets IκBα for proteasome-dependent degradation, releasing NF-κB that can then translocate to the nucleus and regulate gene expression, including that of its own repressor, IκBα (Oeckinghaus and Ghosh, 2009). To determine whether fragment N inhibits IκBα proteolysis, we monitored the pattern of IκBα degradation induced by TNFα in the presence or in the absence of fragment N. Fig. 4A shows that, 30 min after TNFα stimulation, degradation of IκBα took place regardless of whether fragment N was present or not. IκBα expression is regulated by NF-κB and is re-expressed rapidly *de novo* following its degradation (Oeckinghaus and Ghosh, 2009) (see the 60-min and 90-min time points in the control conditions in Fig. 4A). As expected from the ability of fragment N to repress NF-κB activity, IκBα re-expression was inhibited in TNFα-treated cells expressing fragment N (Fig. 4A). Therefore, fragment N does not inhibit IκBα degradation but, as a consequence of fragment-N-mediated NF-κB inhibition, *de novo* synthesis of IκBα is delayed. One mechanism by which fragment N could modulate NF-κB activation is through direct interaction with NF-κB subunits (p50 and p65) in an IκB-like manner. To assess this possibility, the presence of p65 and p50 in fragment N immunoprecipitates was determined. Fig. 4B and C (middle panel blots) show that, in conditions where p65 and p50 co-immunoprecipitated with IκBα, no binding was detected with fragment N. It was possible that fragment N could only interact with NF-κB once it has been freed from IκBα. We therefore repeated the above experiment using cells stimulated with LPS for 45 min or with TNFα for 30 min. In these cases again, no interaction was detected between fragment N and p65 or p50 (supplementary material Fig. S3). These results indicate that IκBα degradation is not modulated by fragment N and that NF-κB dimers are not sequestered in the cytoplasm by direct interaction with fragment N.

Fragment N does not affect NF-κB import but favors nuclear export

To investigate the impact of fragment N on NF-κB nuclear import, nuclear accumulation of GFP–p65 was monitored. As nuclear location of p65 is determined by the balance of nuclear import and nuclear export, we used the nuclear export inhibitor leptomycin B (LMB) (Kudo et al., 1999) to insure that the presence of p65 in the nucleus only depended on nuclear import. Fig. 5 shows that LMB-induced GFP–p65 nuclear accumulation is not modulated by fragment N expression. As a control, a non-degradable 'super-repressor' form of IκBα lacking the IKK-phosphorylation site (IκBαΔN2) completely blocked LMB-induced GFP–p65 nuclear accumulation. These results suggest that fragment N does not affect NF-κB nuclear import.

Given that there is less NF-κB located in the nucleus in cells expressing fragment N (Fig. 3) and because fragment N does not hamper NF-κB nuclear import, one must come to the conclusion that fragment N favors NF-κB nuclear export. To directly test this assertion, fluorescence recovery after photobleaching (FRAP) was

Journal of Cell Science (2015) 128, 3502-3513 doi:10.1242/jcs.174409

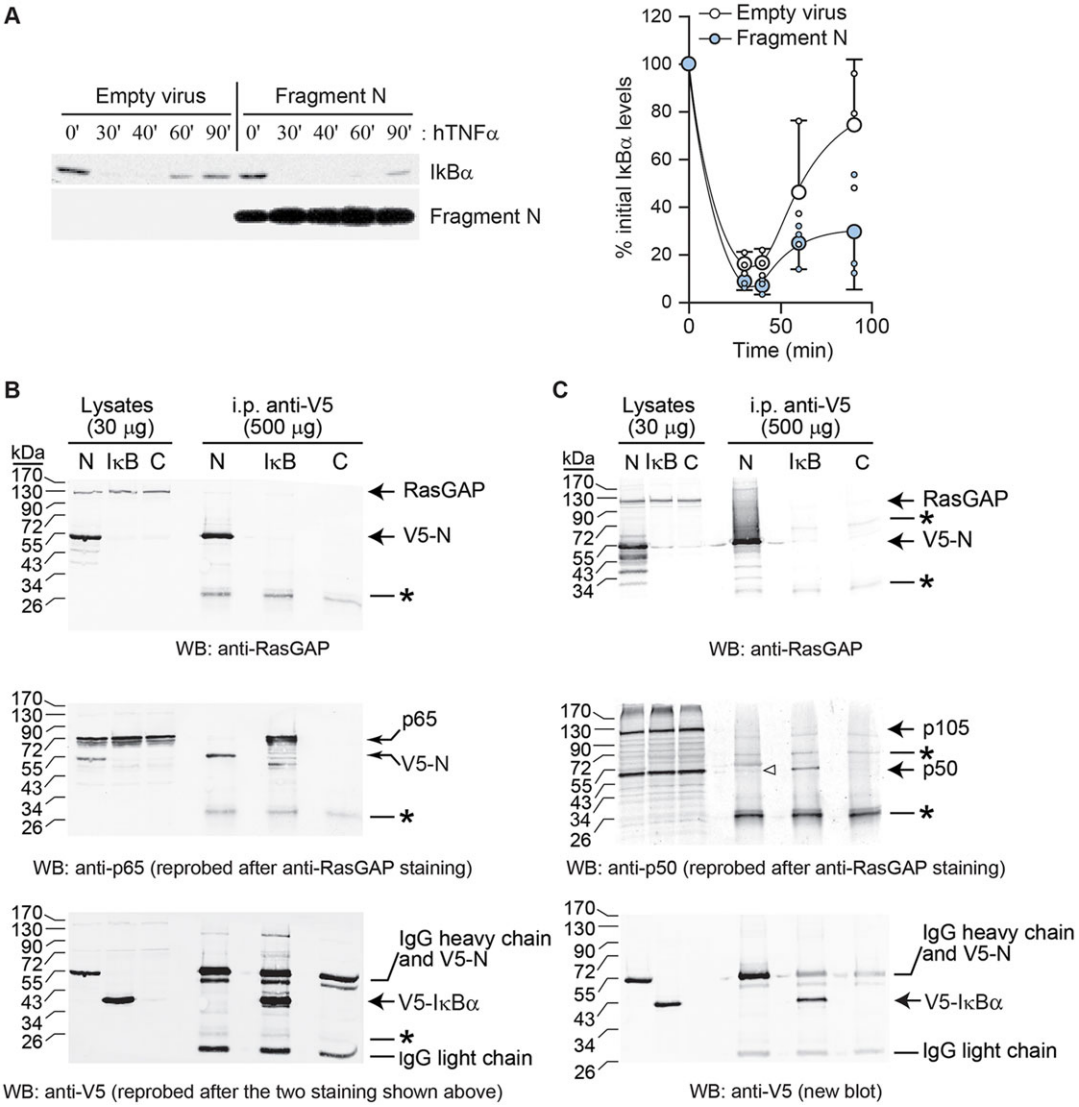

Fig. 4. Fragment N neither inhibits IκBα degradation nor binds to NF-κB. (A) HeLa cells were infected with an empty virus or with an HA-tagged fragment N-encoding virus (N). At 72 h after infection, cells were stimulated for 30 min with 25 ng/ml human (h)TNFα and then lysed in a monoQ-c lysis buffer. The levels of fragment N expression and IκBα were measured by western blotting. Results are shown as mean±95% confidence intervals. (B) 2×10^6 293T cells were transfected with empty pcDNA3, V5-tagged fragment N (V5-N) or V5-tagged IκBα (V5-IκBα) with HA-tagged p65 (HA–p65). 500 μg of cell lysates were then immunoprecipitated with 1 μg of anti-V5 antibody. Lysates and the immunoprecipitated material were analyzed by western blotting. (C) 2×10^6 293T cells were transfected with empty pcDNA3, V5-tagged fragment N (V5-N) or V5-tagged IκBα (V5-IκBα). 500 μg of cell lysates were then immunoprecipitated with 1 μg of anti-V5 antibody. The initial lysates and the immunoprecipitated material were analyzed by western blotting using an anti-RasGAP (upper panel), anti-p50 (middle panel) and anti-V5 antibodies (lower panel). Note that the anti-p50 antibody also recognizes p105. The asterisks in B and C indicate a non-specific band.

performed to monitor nuclear export of GFP-tagged p65 in conditions where fragment N is expressed in cells or not. In control cells, GFP–p65 nuclear export was readily detected but this nuclear export was strongly promoted when cells expressed fragment N (Fig. 6; supplementary material Movie 1). The nuclear membrane integrity of the recorded cells was not affected during FRAP as determined by the total absence of nuclear export of GFP–p65 in the presence of LMB (Fig. 6; supplementary material Movie 1).

Crm1 (also known as XPO1), which is inhibited by LMB, is the main receptor for the export of proteins out of the nucleus and might therefore be targeted by fragment N to increase NF-κB nuclear export (Hutten and Kehlenbach, 2007). However, no interaction between fragment N and Crm1 could be detected (data not shown). Additionally, fragment N did not modulate Crm1 expression levels (supplementary material Fig. S4). Taken together, these results demonstrate that fragment N inhibits NF-κB activity by promoting its export from the nucleus but it does not do so by directly interacting with Crm1.

Repression of NF-κB activity in stressed cells requires caspase activity and fragment N generation

Fragment N is generated in mildly stressed cells in response to a weak caspase-3 activation (Yang et al., 2004). Therefore, based on the data presented above, cells exposed to low stress should have impaired NF-κB activity. However, if caspases are inhibited or if cells are unable to generate fragment N because of a point mutation in the first caspase-3 cleavage site of RasGAP, NF-κB inhibition should not occur. We therefore exposed cells to a low dose of UV-C and tested their capacity to stimulate NF-κB-driven gene expression in response to TNFα. Fig. 7A shows that UV-C pretreatment prevented TNFα-

Journal of Cell Science (2015) 128, 3502-3513 doi:10.1242/jcs.174409

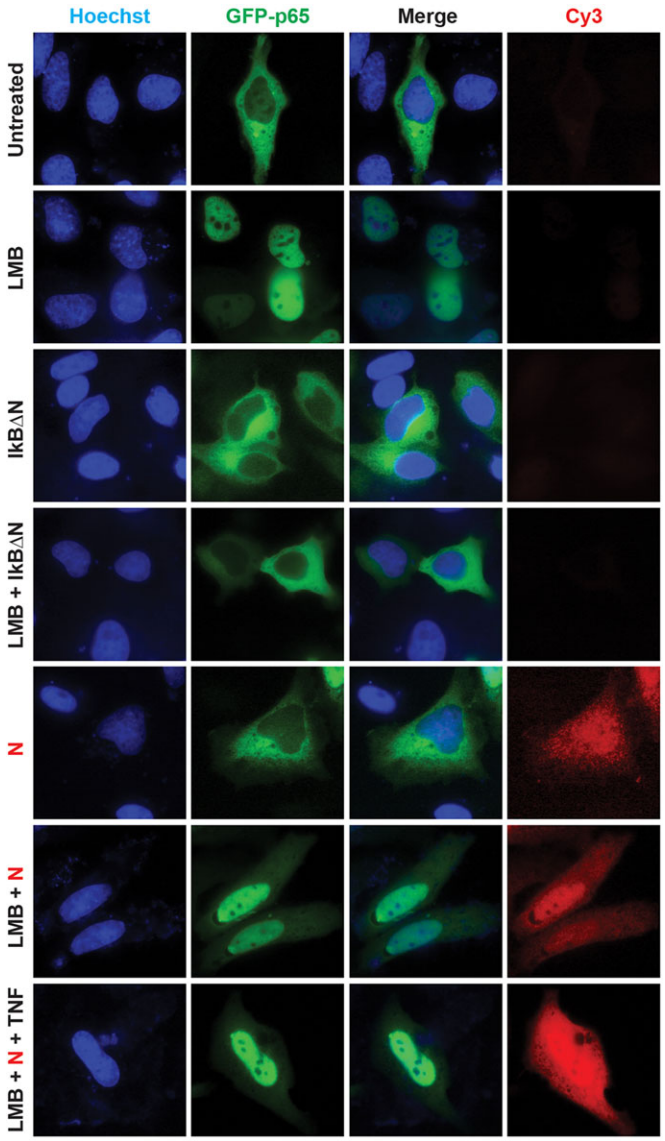

Fig. 5. Fragment N does not inhibit NF-κB nuclear translocation. (A) 250,000 HeLa cells were transfected with an empty plasmid or plasmids encoding an NF-κB super-repressor (IκBαΔN2), fragment N, and GFP in the indicated combinations. After 24 h, the cells were treated with 2 ng/ml of leptomycin B (LMB) for 1 h. The cells were then fixed and processed for immunocytochemistry to detect GFP–p65 and fragment N. Nuclei were stained with Hoechst 33342.

mediated NF-κB activity. However, UV-C pretreatment was unable to prevent NF-κB-driven gene expression when cells were exposed to the pan-caspase MX1013 inhibitor (Jaeschke et al., 2000) (Fig. 7B). This inhibitor has been shown earlier to efficiently prevent RasGAP cleavage and fragment N generation in stressed cells (Yang et al., 2004). Similarly, mouse embryonic fibroblasts (MEFs) that express the D455A RasGAP mutant, which is resistant to caspase-3 cleavage, and hence that are unable to generate fragment N (Fig. 7C, upper part; see also Yang et al., 2004), were still able to induce NF-κB activity despite UV-C pretreatment (Fig. 7C).

Blocking caspase-3-mediated cleavage of RasGAP increased anthralin-induced NF-κB activation in stressed skin

In order to test whether fragment N generation affects NF-κB activity *in vivo*, we used RasGAP$^{D455A/D455A}$ knock-in mice (D455A knock-in mice) that cannot cleave RasGAP due to a mutation at the first caspase-3 cleavage site (Khalil et al., 2012). Note that this mutation also prevents cleavage of RasGAP at the second caspase-3 recognition site (at position 157), presumably because the latter is only exposed when RasGAP is cleaved at the first site (Yang and Widmann, 2001). D455A knock-in mice cannot generate fragment N when they are subjected to various stress stimuli in different organs (Khalil et al., 2012). NF-κB activation in the skin was induced through topical treatment with anthralin, a drug used for the treatment of psoriasis. Anthralin is a pro-oxidant capable of inducing skin inflammation through the elevation of pro-inflammatory cytokines [including IL-6, macrophage inflammatory protein-2 (MIP-2, also known as CXCL2) and TNFα] known to be regulated by NF-κB (Lange et al., 1998; Schmidt et al., 1996).

Wild-type and D455 knock-in mice skin was subjected or not to a low dose (0.05 J/cm^2) of UV-B illumination. This UV-B dose has been shown previously to generate an anti-apoptotic Akt response that is dependent on caspase-3 and fragment N (Khalil et al., 2012). At 24 h after UV-B illumination, NF-κB activation was induced through topical treatment with anthralin. Although leading to clear skin macroscopic changes, UV-B illumination only slightly induced nuclear translocation of NF-κB dimers in keratinocytes (Fig. 8). By contrast, anthralin treatment alone significantly induced nuclear accumulation of NF-κB dimers 6 h after treatment (Fig. 8). In wild-type mice, this response was attenuated by prior UV-B exposure of the skin. In contrast, UV-B illumination was unable to hamper anthralin-induced NF-κB activation in the epidermis of D455A knock-in mice (Fig. 8). These results indicate that the cleavage of RasGAP in response to stress mitigates the NF-κB response in the skin.

DISCUSSION

The NF-κB transcription factor is involved in a variety of important cellular and physiological responses, including modulation of cell survival and the coordination of immune responses (Li and Verma, 2002). The control of NF-κB activity is therefore of considerable importance for tissue homeostasis (Pasparakis, 2009; Viatour et al., 2005). Hence, NF-κB-dependent transcription is tightly controlled, and regulation of its activation is adequately achieved at different levels throughout the NF-κB signaling regulatory cascade (Verma et al., 1995). Human diseases can result from both loss and gain of function in NF-κB signaling. Sustained inhibition of NF-κB is accompanied by severe immune deficiency, increased susceptibility to infection and profound effects on tissue homeostasis in both immune and non-immune cells (Courtois, 2005; Pasparakis, 2009; Wong and Tergaonkar, 2009). Uncontrolled NF-κB activation can lead to chronic inflammation, and increase the risk of cancer, autoimmune diseases (e.g. rheumatoid arthritis), atherosclerosis and neurodegenerative disorders (Ben-Neriah and Karin, 2011; Wong and Tergaonkar, 2009).

NF-κB signaling is mainly regulated through the formation of inhibitory NF-κB–IκB complexes, which impair the nuclear translocation and/or the DNA binding of NF-κB. Few NF-κB cellular inhibitors other than IκB have been identified. These include RelA-associated inhibitor (RAI, also known as PPP1R13L), which directly inhibits the DNA-binding activity of p65 (Yang et al., 1999), and TNF-receptor-associated factors (TRAFs) and NIK-associated protein (TNAP, also known as NCKAP1), which indirectly inhibit p65 phosphorylation and IκB degradation by suppressing NIK kinase activity (Hu et al., 2004). Here, we report that fragment N, a caspase-3-generated cleavage product from the RasGAP protein, is a newly described stress-induced global NF-κB

Journal of Cell Science (2015) 128, 3502-3513 doi:10.1242/jcs.174409

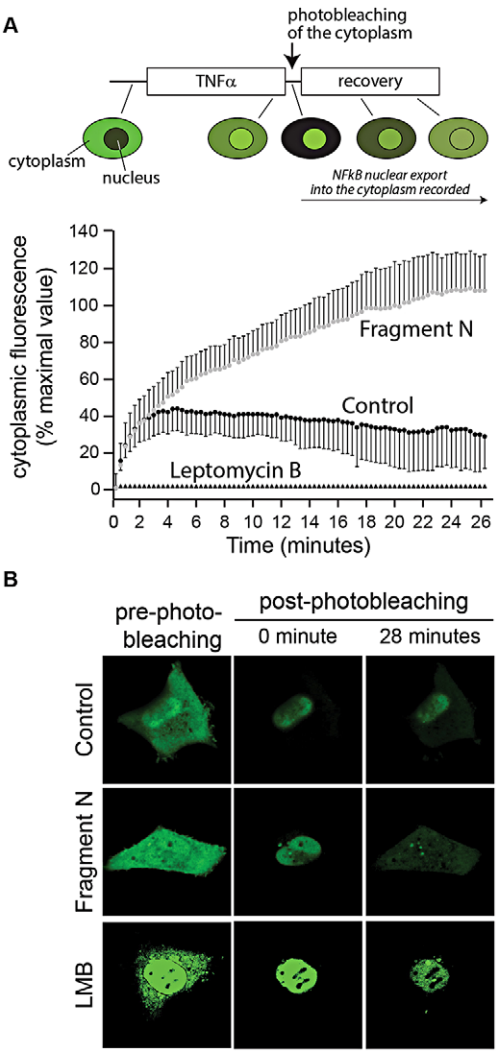

Fig. 6. Fragment N favors NF-κB nuclear export. 250,000 HeLa cells were transfected with an mCherry-encoding plasmid or with an mCherry-tagged fragment N-encoding plasmid together with a GFP–p65-encoding plasmid. Prior to cytoplasmic photo-bleaching, cells were treated for 30 min with human TNFα to promote nuclear accumulation of GFP-tagged p65. Nuclear export of NF-κB was recorded for 28 min by FRAP as indicated in the Materials and Methods section (illustrated schematically in the upper panel of A). When indicated, cells were treated with 2 ng/ml of leptomycin B (LMB) for 1 h prior to TNFα stimulation. Results are shown as mean±95% confidence intervals. (B) Representative images of cells at different times during the FRAP experiment. These images are derived from the time-lapse movie shown in the supplementary material Movie 1. Results are derived from measurements performed on 18 cells per condition from six independent experiments.

inhibitor that acts through its capacity to enhance NF-κB-nuclear export. RasGAP, first identified as a Ras and Rho regulator (Trahey and McCormick, 1987), has been shown to have two caspase-3 cleavage sites used sequentially as cellular stress increases (Wen et al., 1998; Widmann et al., 1998; Yang et al., 2004; Yang and Widmann, 2001). The N-terminal fragment resulting from the first cleavage event on RasGAP (called fragment N) displays strong anti-apoptotic properties by activating the Ras–PI3K–Akt pathway *in vitro* and *in vivo* (Khalil et al., 2012; Yang and Widmann, 2002). We initially reported that fragment-N-mediated Akt stimulation did not result in activation of its downstream effector NF-κB (Yang and Widmann, 2002). In this report, we now show that fragment N acts as a potent NF-κB inhibitor, regardless of the mode of activation of the transcription factor. Indeed, fragment N exerted its inhibitory action in various cell types independently from the mechanism through which NF-κB was induced: activation of upstream kinases (Akt, Cot and NIK), overexpression of key adaptor proteins (TRAF2, TRAF6 and EDAR), or cytokines (Figs 1, 2). These findings indicate that fragment N is a general NF-κB inhibitor, suggesting that it targets an element downstream of these various NF-κB-activating pathways.

Many signaling cascades leading to NF-κB activation converge in a key process, the destruction of IκB, which allows NF-κB to enter the nucleus and regulate gene transcription. IκB degradation is controlled by the IKK complex, and negative regulation of NF-κB could potentially be achieved by targeting this IKK–IκB axis. As shown in Fig. 4, fragment N did not modulate the degradation of IκBα. Neither did fragment N mimic IκBα in sequestering the NF-κB dimers in the cytoplasm, as no binding was detected between fragment N and NF-κB members (Fig. 4). This suggests that the signaling events that trigger NF-κB translocation are not affected by fragment N, consistent with this notion are the data showing that fragment N does not inhibit NF-κB nuclear import (Fig. 5). However, stimulus-triggered nuclear accumulation of NF-κB was found to be decreased by fragment N expression (Fig. 3), and this was associated with an increased NF-κB nuclear export rate (Fig. 6). Fragment N therefore allows less NF-κB dimers to reside in the nucleus, which consequently limits the availability of these dimers to modulate gene expression (e.g. *de novo* synthesis of IκBα; Fig. 4A). Importantly, the NF-κB inhibitory effect seen in cells overexpressing fragment N was also observed in control cells exposed to a mild stress (Fig. 7). In both cases, full NF-κB inhibition was observed. Importantly, this NF-κB inhibitory response induced by stress did not occur in cells genetically modified to express a caspase-resistant RasGAP mutant or in cells in which caspases were inhibited (Fig. 7). Moreover, exposure of the epidermis to a non-cytotoxic mild stress inhibited, in a RasGAP cleavage-dependent manner, further NF-κB activation (Fig. 8). This indicates that the NF-κB blockage controlled by the caspase-3–RasGAP module is a physiologically relevant cellular stress response.

The mechanism by which fragment N favors NF-κB nuclear export has not yet been fully defined. Nuclear export of most proteins requires binding of the proteins to a dimer composed of the Crm1 exportin and the GTP-bound form of Ran (Cook et al., 2007). The formation of this trimeric export complex (protein-cargo–Crm1–Ran-GTP) can be regulated by the Ran-binding protein RanBP3 in two ways. First, RanBP3 brings together the Ran guanine exchange factor RCC1 and Crm1. This induces the GDP-to-GTP exchange on Ran in the export complex (Nemergut et al., 2002). Second, binding of RanBP3 to Crm1 increases the affinity of the latter for its cargos (Englmeier et al., 2001). Phosphorylation of RanBP3 by kinases such as Akt or Rsk stimulates its nuclear export activity (Yoon et al., 2008). Fragment N could favor NF-κB export by targeting the trimeric export complex. However, fragment N did not modulate the expression of Crm1 or RanBP3, nor alter the phosphorylation state of the latter (supplementary material Fig. S4). A direct influence of fragment N on the export machinery, if any, therefore remains to be characterized.

As indicated in the introduction, NF-κB can be regulated by caspases but this seems often to happen independently of the proteolytic activity of the enzyme (Chaudhary et al., 2000; Kreuz et al., 2004; Lamkanfi et al., 2005). Nevertheless, there are a few cases where caspase activity is involved in NF-κB regulation. For example, caspase-1-mediated cleavage of Lyn generates a

Journal of Cell Science (2015) 128, 3502-3513 doi:10.1242/jcs.174409

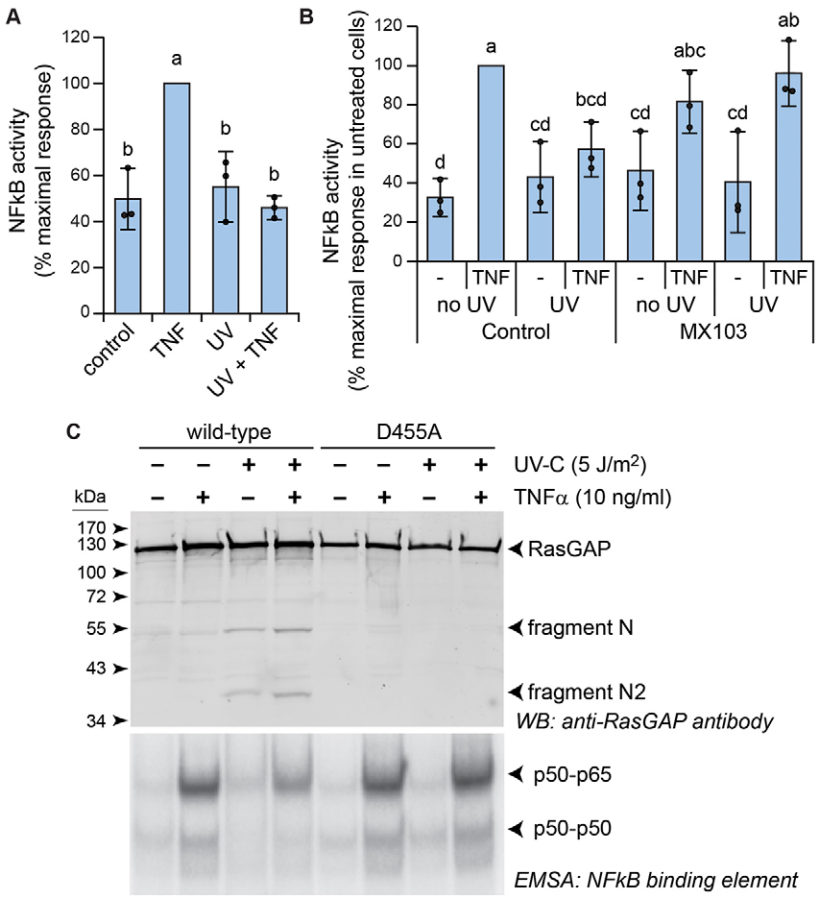

Fig. 7. Stress that induces the formation of fragment N inhibits NF-κB activation in a caspase-dependent manner. (A) HeLa cells were transfected with the prLUC NF-κB reporter. After 1 day, the cells were illuminated or not with UV-C (46 J/m^2) and, after a 24 h additional period of time, the cells were stimulated or not for 30 min with 25 ng/ml of human TNFα. NF-κB activity was then determined as described in Fig. 2A (three experiments performed in duplicate). (B) HeLa cells were transfected as described in Fig. 1A. The cells were then pre-incubated or not with 10 μM of the MX1013 pan-caspase inhibitor for 6 h, followed by UV illumination and TNFα stimulation as described in A. NF-κB activity was then determined as described in Fig. 2A. Results are shown as mean±95% confidence intervals and are statistically different (P<0.05) when indicated with different lowercase letters. (C) Wild-type or RasGAP D455A MEFs (i.e. MEFs that express a caspase-resistant form of RasGAP) were treated as described in A. Cells were then lysed and the pattern of RasGAP cleavage was analyzed by western blotting (WB) using a RasGAP antibody able to detect full-length as well as fragments N and N2 (upper panel). Alternatively, the extent of NF-κB activation was monitored by EMSA (lower panel).

fragment (LynΔN) that inhibits NF-κB activation (Marchetti et al., 2009). Moreover, cleavage of PARP by caspase-3 has been reported to induce NF-κB activation, but the underlying mechanisms are still ill defined (Lamkanfi et al., 2007). In contrast, our present finding suggests that caspase-3, through the generation of fragment N, inhibits NF-κB activation. Why would

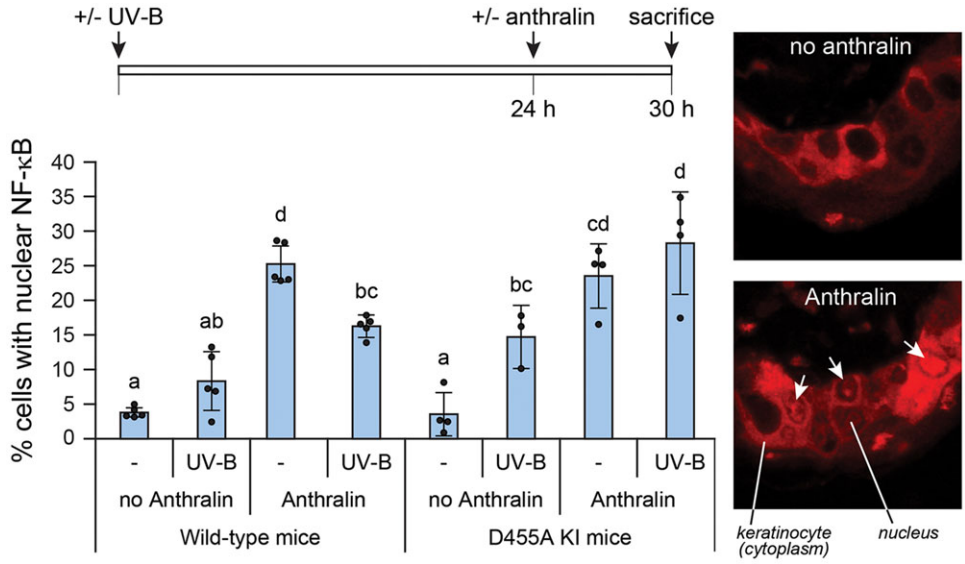

Fig. 8. Stress does not regulate NF-κB activation in the skin of D455A knock-in mice that are unable to cleave RasGAP into fragment N. Eight-week-old mice were shaved and 24 h later were anaesthetized and illuminated with 0.05 J/cm^2 UV-B as indicated in the Materials and Methods section. Only one side of the mouse was illuminated and the other side was used as a control (i.e. non-UV-B illuminated). At 24 h after illumination, mice skin was topically treated or not with 20 mM anthralin for 6 h. At the end of the 6 h treatment, the mice were killed and lateral skin biopsies were excised and processed for anti-p65 staining on paraffin slices. The percentage of keratinocytes with prominent nuclear localized p65 (see white arrows on the images shown on the right-hand side) was determined (3–5 samples, derived from a total of 25 mice, were analyzed per condition). Results are shown as mean±95% confidence intervals and are statistically different (P<0.05) when indicated with different lowercase letters. KI, knock-in.

Journal of Cell Science (2015) 128, 3502-3513 doi:10.1242/jcs.174409

caspase-3 generate cleavage fragments with opposite regulatory functions on NF-κB activity? One potential explanation to resolve this apparent conundrum is that fragment N is produced at low caspase-3 activities. Higher activities, necessary for the processing of PARP, also lead to further processing of fragment N and the loss of its activity (Yang et al., 2004). Therefore, the manner by which caspase-3 modulates NF-κB might vary drastically at different cellular stress intensities.

Our earlier data describing the capacity of the caspase-3 and RasGAP module to induce an anti-death Akt-dependent program in stressed cells (reviewed in Khalil et al., 2014) provided a molecular basis for hormesis, the protective response induced in cells and organisms exposed to low doses of toxic compounds (Calabrese et al., 2010). The present data expand the potential beneficial effect of the caspase-3–RasGAP stress sensor to the control of NF-κB activation, a key event in the regulation of tissue inflammation (Lawrence, 2009). Inflammation is generally beneficial for an organism exposed to injury or acute infection. An optimal (i.e. maximal NF-κB response) might be appropriate and beneficial in non-stressed organisms but could become detrimental in organisms exposed to earlier stress conditions or stimuli, as suggested, for example, in leprosy and psoriasis (Bakry et al., 2014; Wambier et al., 2014). In such cases, dampening the potential to activate NF-κB in response to a later infection or injury might become advantageous. Further work will be required to determine precisely the participation of the caspase-3–RasGAP module in the control of such inflammatory responses. In this context, it is interesting to mention that drugs, such as corticosteroids, aspirin and other non-steroidal anti-inflammatory drugs (NSAIDs), which are used to treat inflammatory diseases, nonspecifically affect NF-κB activity (Yamamoto and Gaynor, 2001). Our data suggest that the efficacy of anti-inflammatory drugs might be increased if caspases are not simultaneously inhibited by these drugs.

MATERIALS AND METHODS

Plasmid descriptions

dn3, *cmv*, *cr3* and *rk5* after the plasmid name indicates that the backbone vector is pcDNA3 (Invitrogen, catalog no. A-150228), pCMV4/5 (Promega, Madison, WI), pCR3 (Invitrogen, catalog no. V1.0-140711sa), and pRK-5 (BD Pharmingen, Franklin Lakes, NJ, catalog no. 556104), respectively. pmCherry-N1 and pEGFP-C1 encoding for red and green fluorescent proteins, were from Clontech (catalog no. 632523 and 6084-1, respectively). pRL-TK encodes the *Renilla reniformis* luciferase (Promega, catalog no. E2241). prLUC is an NF-κB reporter plasmid, with two NF-κB responsive elements and a minimal cFos promoter upstream of the firefly luciferase (Bulat et al., 2011). h-H-Ras(G12V).dn3 encodes a constitutively active H-Ras (described previously as V12Ras.dn3; Yang and Widmann, 2002). h-H-Ras(S17N).cmv encodes a dominant-negative H-Ras (described previously as N17Ras.cmv; Yang and Widmann, 2001). HA-hRasGAP[1-455](D157A).dn3 encodes the HA (MGYPYDVPDYAS)-tagged, caspase-resistant form of RasGAP fragment N (amino acids 1–455, described previously as N-D157A.dn3; Yang and Widmann, 2001). HA-hRasGAP[1-455](D157A).lti is a lentiviral vector encoding the uncleavable form of fragment N (described previously as N-D157A.lti; Yang et al., 2005a). V5-hRasGAP[3-455](D157A).dn3 encodes the V5 (MGKPIPNPLLGLDST)-tagged version of the caspase-resistant form of fragment N lacking the first two amino acids (Annibaldi et al., 2011). HA-hRasGAP[1-455](D157A)-no stop.dn3 bears the HA-tagged version of caspase-resistant fragment N lacking the stop codon. It was constructed by PCR amplifying HA-hRasGAP[1-455](D157A).dn3 with the sense oligonucleotide no. 71 (5′-GCGTGGATAGCGGTTTGACTC-3′) and the anti-sense oligonucleotide no. 333 (5′-AAAAAAAAGCGGCCGCGTCGACTGTGTCATTGAGTA-C-3′). The PCR fragment was then cut with Bsu36 and NotI and the resulting 784-bp fragment subcloned into HA-hRasGAP[1-455](D157A). dn3 opened with the same enzyme. HA-hRasGAP[1-455](D157A)-mCherry.dn3 encodes a fusion protein between the HA-tagged version of caspase-resistant fragment N and the fluorescent protein mCherry. It was constructed by PCR amplification of pmCherry-N1 with the sense oligonucleotide no. 813 (5′-AAAAAACTCGAGCCATGGTGAGCAA-GGGCGAGGA-3′) and the anti-sense oligonucleotide no. 816 (5′-TTT-TTTTCTAGACTACTTGTACAGCTCGTCCATGCCGCC-3′). The resulting PCR product was digested with XhoI and XbaI and inserted into plasmid HA-hRasGAP[1-455](D157A)-no stop.dn3 cut with the same enzyme. HA-hRasGAP(D455A).dn3 encodes an N-terminally HA-tagged version of human p120 RasGAP bearing an aspartate to alanine mutation at position 455 (described previously as HA-D455A.dn3 (Yang and Widmann, 2001). myr-mAkt1-HA.cmv encodes a constitutively active form of Akt that bears an N-terminal Src myristoylation sequence (MGSSKSKPK) and a C-terminal HA tag (described previously as myr-Akt.cmv; Yang and Widmann, 2002). hIkB alpha.tb7 bears the human IκBα cDNA [nucleotides 2–1448 (Genbank NM_020529), with T1228C and G1535C mutations in the 3′ untranslated region]. It was obtained from RZPD (Deutsches Ressourcenzentrum for Genomforschung, catalog no. IRAUp969B0119D6). hIkB alpha.dn3 contains the same insert of hIkB alpha.tb7 but placed in the pcDNA3 eukaryotic expression vector. It was constructed by sub-cloning the blunted SmaI/BamHI hIkB alpha.tb7 fragment into pcDNA3 opened with the same enzymes and blunted. V5-hIkB alpha.dn3 encodes a V5-tagged version of human IκBα. It was constructed by PCR amplification of plasmid hIkB alpha.dn3 with the sense oligonucleotide no. 653 (5′-CGCGGATCCGCCACCATGGGCAAGCC-AATCCCTAATCCACTCCTCGGCCTCGACAGTACTATGTTCCAGG-CGGCC-3′) and the anti-sense oligonucleotide no. 677 (5′-AAAAAA-GAAGTGCCTCAGCAATTTCTGGCT-3′). The resulting 441-bp PCR product was digested with BamHI and BbvCI and inserted into plasmid hIκB alpha.dn3 that was linearized with the same restriction enzymes. hIκB alpha delta N2.cmv encodes the human IκBα protein with the ΔN2 deletion (i.e. amino acids 3–71). This construct cannot be phosphorylated by IκB kinases and degraded by the proteasome and therefore functions as an inhibitor of NF-κB. It has been described previously under the name of IκBαΔN2 (Yang and Widmann, 2002). V5-hIkB alpha delta N2.mCherry was constructed by PCR amplifying hIkB alpha delta N2.cmv with oligonucleotide #814 (5′-AAAAAACTCGAGGCCACCATGGGAAAA-CCAATACCAAATCCACTACTAGGCCTAGACAGTACAATGTTCGA-GGACGGGGACTCG-3′) and oligonucleotide #815 (5′-AAAAAAGGA-TCCGCTGCTAACGTCAGACGCTGGCCTCCAA-3′). The resulting 818 bp PCR product was digested with BamHI and XhoI and inserted into plasmid pmCherry-N1 that was linearized with the same restriction enzymes. myc-hRelA.cr3 encodes a myc (EQKLISEEDL)-tagged version of human RelA, with an NRSPGEFCRYP-coding intervening sequence in-between. GFP-hRelA.dn3 encodes a fusion protein between the GFP and human RelA. For its construction, the myc-hRelA.dn3 plasmid was digested with XhoI, blunt-ended with Klenow, and then digested with HindIII. The resulting 1780-bp fragment was inserted into pEGFP-C3 opened with BamHI, blunt-ended with Klenow and then digested with HindIII. The resulting plasmid (GFP-stop-myc-hRelA) contains a stop codon between the GFP- and the myc-coding sequences. Both were removed by a ScaI and EcoRV digestion and self-ligation, generating plasmid GFP-hRelA.dn3. hNIK-HA.cmv, which encodes the human NF-κB-inducing kinase (NIK) bearing a C-terminal HA tag. FLAG-hTRAF2.cr3 encodes the human TRAF2 protein (nucleotides 64–1563 of Genbank BC043492; first 2 codons missing) bearing an N-terminal FLAG tag (MDYKDDDDK). FLAG-mTRAF6.dn3 encodes the mouse TRAF6 protein (nucleotides 371–1999 of NCBI entry NM_009424) bearing an N-terminal FLAG tag. mEDAR.dn3 encodes the mouse ectodysplasin A receptor cDNA (nucleotides 260–1604, Genbank NM_010100). myc-hCot.rk5 bears a myc-tagged form of human Cot. 3xFlag-hCRM1.cmv is a plasmid encoding a Flag-tagged form of human Crm1 (Addgene 17647).

Cells and transfection

HEK 293 cells (ATCC, Manassas, VA, CRL-1573) were grown in DMEM medium (GIBCO, Life Technologies, Carlsbad, CA; catalog no. 61965) supplemented with 10% fetal calf serum (Invitrogen, Life Technologies,

Journal of Cell Science (2015) 128, 3502-3513 doi:10.1242/jcs.174409

catalog no. 41Q2174K), 100 units/ml penicillin, and 0.1 mg/ml streptomycin (Sigma-Aldrich, St Louis, MO, catalog no. P0781). HeLa and INS1 cells were maintained in RPMI-1640 (GIBCO #61870-10) containing 10% fetal calf serum, supplemented with 50 µM β-mercaptoethanol for INS-1 cells. All these cells were cultured at 37°C and 5% CO_2. INS1 and HeLa cells were transfected with the indicated plasmids using Lipofectamine 2000 (Life Technologies; catalog no. 11668-019). HEK 293 cells were transfected using the calcium phosphate precipitation procedure (Jordan et al., 1996). At 8 h after transfection, the medium containing the DNA precipitates was replaced with fresh serum-containing culture medium.

Chemicals and antibodies

Human TNFα was from Roche (Basel, Switzerland, catalog no. 11-088-939-001). Mouse recombinant IL1β and lipopolysaccharide (LPS) were from Sigma-Aldrich (catalog no. I5271 and L6529 respectively). Leptomycin B was from Calbiochem (Merck Millipore, Billerica, MA; catalog no. 431050). Hoechst 33342 was from Roche (catalog no. H-1399). It was diluted in water at a final concentration of 10 mg/ml and stored at 4°C in the dark. The pan-caspase inhibitor MX1013 (quinolyl-valyl-O-methylaspartyl[2,6-difluorophenoxy]-methyl ketone, Q-VD-OPh), was from MP Biomedicals (Santa Ana, CA; catalog no. OPH109). Anthralin was from Santa Cruz Biotechnology (Dallas, TX; catalog no. sc-202466). Mouse anti-V5 antibody was from Invitrogen (catalog no. R960-25). Rabbit anti-V5 antibody, and anti-Crm1 and anti-total RanBP3 antibodies were from Abcam (Cambridge, UK; catalog nos 15828, ab24189 and ab2939, respectively). HA-tag-specific antibodies were purchased as ascites from Babco (Richmond, CA; catalog no. MMS-101R). This antibody was adsorbed on HeLa cell lysates to decrease non-specific binding as previously described (Yang and Widmann, 2001). The anti-RasGAP antibody was from Enzo Life Science (Lausen, Switzerland, catalog no. ALX-210-860-R100) and is directed at the fragment N2 moiety of the human protein (amino acids 158–455). The rabbit polyclonal IgG antibody recognizing Akt1 and Akt2 was from Santa Cruz Biotechnology (catalog no. SC-8312). The anti-IκBα, anti-p50 and p105, anti-p65 and the phospho-specific anti-RanBP3 (serine 58) and anti-Akt (serine 473) antibodies were from Cell Signaling (Danvers, MA; catalog nos 9242, 3035, 3034, 9380 and 9271, respectively). The anti-p65 rabbit polyclonal antibody used in skin experiments was from Santa Cruz biotechnology (catalog no. sc-372). The secondary antibody used in immunocytochemistry experiments was a Cy3-conjugated AffiniPure Goat anti-mouse IgG (H+L) from Jackson ImmunoResearch Laboratories (West Grove, PA; 115-165-146). Alexa-Fluor-680-conjugated goat anti-rabbit-IgG (H+L) (Molecular Probes, Eugene, OR; A21109) and IRDye-800-conjugated affinity purified anti-mouse-IgG (H+L) (Rockland, Limerick, PA; 610-132-121) were the secondary antibodies used for western blots. The anti-tubulin antibody was from Genetex (Irvine, CA; GTX628802).

Quantification of the percentage of nuclear GFP–p65

Quantification of the nuclear GFP–p65 was performed by measuring the mean intensity of GFP fluorescence in cytoplasm and in the nucleus then calculating the ratio using ImageJ software.

Fluorescence recovery after photobleaching

A total of 200,000 HeLa cells were seeded in 35-mm glass-bottomed micro-well dishes (MatTek, catalog no P35G-1.5-14-C). After 24 h, the cells were co-transfected with the indicated plasmids. After an additional 24-h period, the cells were treated for 30 min with human TNFα to promote GFP–p65 nuclear accumulation. FRAP was then performed using a LSM710 Zeiss confocal microscope (Carl Zeiss, Oberkochen, Germany) piloted by the ZEN 2009 software and equipped with a 40× objective (EC Plan-neofluar 40×1.30 NA Oil DIC M27). Photo-bleaching was achieved by simultaneous laser excitation at three wavelengths 458, 488 and 514 nm for 20 s. Cytoplasmic fluorescence recovery was recorded by the ZEN 2009 software (one image was taken every 20 s during the whole duration of the experiments). The cytoplasmic intensity values (i.e. the total fluorescence intensity values in the whole cytoplasmic surface) were normalized to the nuclear fluorescence intensity at time 0 (i.e. the nuclear value found in the first image recorded after photobleaching). For a given experiment, the resulting ratios were normalized to the maximal recorded ratio, which in the present study is obtained when cells express fragment N.

NF-κB luciferase reporter assay

Cells cultured in six-well plates were transfected with the plasmids of interest in the presence of 0.25 µg of prLUC, an NF-κB firefly luciferase reporter (Bulat et al., 2011) and 0.25 µg of pRL-TK, encoding the *Renilla* luciferase. The total amount of DNA used in the transfection was always kept to 3 µg by the addition of empty pcDNA3 when required. Luciferase assay was performed using the Dual-Luciferase Reporter Assay from Promega (E1910). At 24 h after transfection, the cells were lysed in 200 µl of passive lysis buffer. In some cases, the cells were treated for 30 min with TNFα or IL1β before lysis. The firefly luciferase activity was recorded by mixing 25 µl of the lysate with 25 µl of the LARII Reagent and the *Renilla* luciferase activity was recorded by adding to the previous mix 25 µl of the Stop and Glo reagent. For each measurement, light emission was quantified during 12 s using a Lumat LB 9501 luminometer (Berthold Technologies, Zurich, Switzerland). Results are expressed as the ratio of the firefly luciferase signal to the *Renilla* luciferase signal.

Akt kinase assay

HeLa cells were cultured and transfected with the indicated plasmids. Cells were then starved for 48 h and the Akt kinase activity was measured using a kinase assay from Cell Signaling (catalog no. 9840) as per the manufacturer's instructions. Cells were lysed in 0.5 ml monoQ-c buffer (70 mM β-glycerophosphate, 0.5% Triton X-100, 2 mM $MgCl_2$, 100 mM Na_3VO_4, 1 mM dithiothreitol, 20 µg/ml aprotinin) (Yang and Widmann, 2001). The lysates were cleared by centrifugation at 16,000 ***g*** for 15 min, and 300 µg of cell lysate proteins were used for Akt immunoprecipitation.

Western blot analysis

Cells were lysed in monoQ-c buffer and protein quantification was performed by the Bradford technique. Equal amounts of proteins were subjected to SDS-PAGE and then transferred onto a nitrocellulose membrane (Biorad, Hercules, CA; catalog no. 162-0115). The membranes were blocked with TBS containing 0.1% Tween 20 (TBST) and 5% non-fat milk and incubated overnight at 4°C with the primary antibodies. Blots were then washed with TBST, incubated with the appropriate secondary antibody (1:5000 dilution) for 1 h at room temperature and subsequently visualized and quantified with the Odyssey infrared imaging system (LICOR Biosciences, Bad Homburg, Germany). When stripped and reprobed, blots were incubated at 50°C for 30 min in stripping buffer (62.5 mM Tris-HCl pH 6.7, 100 mM β-mercaptoethanol, 1% SDS) followed by three 20-min long washes at room temperature in TBST.

Immunocytochemistry

Cells were grown on glass coverslips. After the specified transfection and treatment, the cells were fixed and immunocytochemistry was performed as previously described (Annibaldi et al., 2009).

Immunoprecipitation

A total of 2×10^6 HEK 293T cells were seeded in 10-cm plates and the following day transfected using the calcium phosphate precipitation procedure (Jordan et al., 1996). After 24 h, cells were lysed in lysis buffer (50 mM Tris-HCl pH 7.4, 150 mM NaCl and 1% NP-40) and 500 µg of the lysate proteins were incubated with 1 µg of the specified antibody for 12 h at 4°C. 30 µl of G sephrose beads (Amersham, GE Healthcare, Little Chalfont, UK; catalog no. 17-0618-01) were then added to the samples and the incubation resumed for an additional 2 h. Immunoprecipitate complexes were then washed three times with PBS and solubilized in 30 µl sample buffer (250 mM Tris-HCl pH 7, 10% SDS, 30% glycerol and 5% β-mercaptoethanol) and subjected to SDS-PAGE.

Electrophoretic mobility shift assay

Cells were washed in ice-cold PBS and then resuspended in buffer A (10 mM Hepes pH 7.9, 10 mM KCl, 0.1 mM EDTA, 0.1 mM EGTA, 1 mM dithiothreitol, 1 mM phenylmethylsulfonyl fluoride [PMSF]) (400 µl/well for 6-well plates). Cells were kept on ice for 15 min, then 12.5 µl of 10%

NP40 was added, and the cells were pelleted for 2 min at 16,000 ***g***. The pellet was washed with 100 µl of buffer A and resuspended in 50 µl buffer C (20 mM Hepes pH 7.9, 0.4 M NaCl, 1 mM EDTA, 1 mM EGTA, 1 mM dithiothreitol, 1 mM PMSF). After 20 min of incubation on ice, the cells were centrifuged for 5 min at 16,000 ***g***, and the supernatants (nuclear extracts) were transferred to a new tube and frozen at −80°C. A probe containing an NF-κB-binding site (underlined) was prepared by annealing the complementary nucleotides 5′-GGCAGTTGAAGGGGACTTTCCC-AGG-3′ and 5′-GGTAGCCTGGGAAAGTCCCCTTCA-3′. The annealed probe was labeled with [^{32}P]dCTP (5 µCi) using Klenow DNA polymerase (2 U/µl; Promega cat. no. M2201). 4 ng of the labeled probe and 10 µg of nuclear extracts were mixed in an equal volume of 2× binding buffer [20 mM Hepes pH 7.9, 50 mM KCl, 0.5 mM EDTA, 0.1% NP40, 1 mg/ml BSA, 10% glycerol and 0.4 µg/µl poly(deoxyinosine-deoxycytidine) (Amersham bioscience, cat. no. 27-7880-01), 2 mM PMSF, 2 mM DTT], incubated at room temperature for 20 min, and then separated in a 0.5× TBE, 5% polyacrylamide native gel. The dried gel was analyzed using a Phosphoimager (Bio-Rad).

Lentiviral infection

Recombinant lentiviruses were produced as described previously (Yang et al., 2005a).

UV-B exposure, anthralin treatment and isolation of skin samples

Mice were shaved on both flanks followed by depilation with a depilatory cream (Veet). After 24 h, the mice were anesthetized and illuminated or not with a Waldmann UV apparatus equipped with a Philips UV21 UV-B lamp (TL 20W/12RS). The dose of UV-B illumination, measured with a Waldmann Variocontrol dosimeter, was 0.05 J/cm^2. Anthralin was dissolved in chloroform at a stock concentration of 125 mM. For the experiments, anthralin was freshly diluted in a mixture of 70% ethanol/olive oil (4:1). In each case, one side of the mouse was topically treated for 6 h with anthralin (10 µl of a 20 mM solution spread on a 3–4 cm^2 shaved skin surface) and the other side was used as a control (i.e. treated with vehicle only). Mice were killed after 6 h. Lateral skin biopsies (approximately 2 cm^2) were excised from each mouse, fixed in PBS, 4% formol solution, and embedded in paraffin. The paraffin-embedded skin was cut into 4 µm sections, deparaffinized and stained with anti-p65 for histological observation. All animal experiments were performed according to approved guidelines.

Statistical analysis

The statistical analyses used in this study were one-way ANOVAs performed with the SAS 9.2 TS Level 2M0 software (SAS Institute Inc., Cary, NC). Lowercase letters were used in the figures to display the results of the statistical tests. When means are labeled with the same letter(s), they are not significantly different. When not displayed as box plots, results are shown as mean±95% confidence intervals and the individual points are displayed (when n<10) (Weissgerber et al., 2015).

Acknowledgements

We thank the late Jürg Tschopp, Fabio Martinon and Arthur Weiss for the gift of plasmids myc-hRelA.cr3, hNIK-HA.cmv, and Myc-hCot.rk5, respectively. We thank David Barras for the preparation of the movie shown in the supplementary material.

Competing interests

The authors declare no competing or financial interests.

Author contributions

H.K., N.L. and C.W. designed the study; H.K., N.L., A.R. A.C.-M. and E.S. performed the experiments; H.K., A.C.-M., M.H. and C.W. analyzed the data; H.K. and C.W. wrote the paper with input from A.C.-M., N.L. and M.H.

Funding

This work was supported by grants from the Swiss National Science Foundation [grant numbers 3100-066797, 3100A0-107819, 3100A0-119876 and 31003A_141242/1 to C.W.].

Supplementary material

Supplementary material available online at
http://jcs.biologists.org/lookup/suppl/doi:10.1242/jcs.174409/-/DC1

References

Annibaldi, A., Michod, D., Vanetta, L., Cruchet, S., Nicod, P., Dubuis, G., Bonvin, C. and Widmann, C. (2009). Role of the sub-cellular localization of RasGAP fragment N2 for its ability to sensitize cancer cells to genotoxin-induced apoptosis. *Exp. Cell Res.* **315**, 2081-2091.

Annibaldi, A., Dousse, A., Martin, S., Tazi, J. and Widmann, C. (2011). Revisiting G3BP1 as a RasGAP binding protein: sensitization of tumor cells to chemotherapy by the RasGAP 3127-326 sequence does not involve G3BP1. *PLoS ONE* **6**, e29024.

Baker, R. G., Hayden, M. S. and Ghosh, S. (2011). NF-κB, inflammation, and metabolic disease. *Cell Metab.* **13**, 11-22.

Bakry, O. A., Samaka, R. M., Shoeib, M. A. and Abdel Aal, S. M. (2014). Nuclear factor kappa B and cyclo-oxygenase-2: two concordant players in psoriasis pathogenesis. *Ultrastruct. Pathol.*, **39**, 1-13.

Baldwin, A. S., Jr. (1996). The NF-kappa B and I kappa B proteins: new discoveries and insights. *Annu. Rev. Immunol.* **14**, 649-681.

Barnes, P. J. (1997). Nuclear factor-kappa B. *Int. J. Biochem. Cell Biol.* **29**, 867-870.

Ben-Neriah, Y. (2002). Regulatory functions of ubiquitination in the immune system. *Nat. Immunol.* **3**, 20-26.

Ben-Neriah, Y. and Karin, M. (2011). Inflammation meets cancer, with NF-κB as the matchmaker. *Nat. Immunol.* **12**, 715-723.

Bonizzi, G. and Karin, M. (2004). The two NF-kappaB activation pathways and their role in innate and adaptive immunity. *Trends Immunol.* **25**, 280-288.

Bulat, N., Jaccard, E., Peltzer, N., Khalil, H., Yang, J.-Y., Dubuis, G. and Widmann, C. (2011). RasGAP-derived fragment N increases the resistance of beta cells towards apoptosis in NOD mice and delays the progression from mild to overt diabetes. *PLoS ONE* **6**, e22609.

Calabrese, V., Cornelius, C., Dinkova-Kostova, A. T., Calabrese, E. J. and Mattson, M. P. (2010). Cellular stress responses, the hormesis paradigm, and vitagenes: novel targets for therapeutic intervention in neurodegenerative disorders. *Antioxid. Redox. Signal.* **13**, 1763-1811.

Chaudhary, P. M., Eby, M. T., Jasmin, A., Kumar, A., Liu, L. and Hood, L. (2000). Activation of the NF-kappaB pathway by caspase 8 and its homologs. *Oncogene* **19**, 4451-4460.

Chung, J. Y., Park, Y. C., Ye, H. and Wu, H. (2002). All TRAFs are not created equal: common and distinct molecular mechanisms of TRAF-mediated signal transduction. *J. Cell Sci.* **115**, 679-688.

Cook, A., Bono, F., Jinek, M. and Conti, E. (2007). Structural biology of nucleocytoplasmic transport. *Annu. Rev. Biochem.* **76**, 647-671.

Courtois, G. (2005). The NF-κB signaling pathway in human genetic diseases. *Cell. Mol. Life Sci.* **62**, 1682-1691.

Cross, D. A. E., Alessi, D. R., Cohen, P., Andjelkovich, M. and Hemmings, B. A. (1995). Inhibition of glycogen synthase kinase-3 by insulin mediated by protein kinase B. *Nature* **378**, 785-789.

Darding, M. and Meier, P. (2012). IAPs: guardians of RIPK1. *Cell Death. Differ.* **19**, 58-66.

Englmeier, L., Fornerod, M., Bischoff, F. R., Petosa, C., Mattaj, I. W. and Kutay, U. (2001). RanBP3 influences interactions between CRM1 and its nuclear protein export substrates. *EMBO Rep.* **2**, 926-932.

Gardam, S. and Brink, R. (2014). Non-canonical NF-κB signaling Initiated by BAFF influences B cell biology at multiple junctures. *Front. Immunol.* **4**, 509.

Gerondakis, S., Fulford, T. S., Messina, N. L. and Grumont, R. J. (2014). NF-κB control of T cell development. *Nat. Immunol.* **15**, 15-25.

Hu, W.-H., Mo, X.-M., Walters, W. M., Brambilla, R. and Bethea, J. R. (2004). TNAP, a novel repressor of NF-kappaB-inducing kinase, suppresses NF-kappaB activation. *J. Biol. Chem.* **279**, 35975-35983.

Hutten, S. and Kehlenbach, R. H. (2007). CRM1-mediated nuclear export: to the pore and beyond. *Trends Cell Biol.* **17**, 193-201.

Jaeschke, H., Farhood, A., Cai, S. X., Tseng, B. Y. and Bajt, M. L. (2000). Protection against TNF-induced liver parenchymal cell apoptosis during endotoxemia by a novel caspase inhibitor in mice. *Toxicol. Appl. Pharmacol.* **169**, 77-83.

Jordan, M., Schallhorn, A. and Wurm, F. M. (1996). Transfecting mammalian cells: optimization of critical parameters affecting calcium-phosphate precipitate formation. *Nucleic Acids Res.* **24**, 596-601.

Kane, L. P., Mollenauer, M. N., Xu, Z., Turck, C. W. and Weiss, A. (2002). Akt-dependent phosphorylation specifically regulates Cot induction of NF-kappa B-dependent transcription. *Mol. Cell. Biol.* **22**, 5962-5974.

Khalil, H., Peltzer, N., Walicki, J., Yang, J.-Y., Dubuis, G., Gardiol, N., Held, W., Bigliardi, P., Marsland, B., Liaudet, L. et al. (2012). Caspase-3 protects stressed organs against cell death. *Mol. Cell. Biol.* **32**, 4523-4533.

Khalil, H., Bertrand, M. J. M., Vandenabeele, P. and Widmann, C. (2014). Caspase-3 and RasGAP: a stress-sensing survival/demise switch. *Trends Cell Biol.* **24**, 83-89.

Kopp, E. B. and Ghosh, S. (1995). NF-kappa B and rel proteins in innate immunity. *Adv. Immunol.* **58**, 1-27.
Kreuz, S., Siegmund, D., Rumpf, J.-J., Samel, D., Leverkus, M., Janssen, O., Hacker, G., Dittrich-Breiholz, O., Kracht, M., Scheurich, P. et al. (2004). NFκB activation by Fas is mediated through FADD, caspase-8, and RIP and is inhibited by FLIP. *J. Cell Biol.* **166**, 369-380.
Kudo, N., Matsumori, N., Taoka, H., Fujiwara, D., Schreiner, E. P., Wolff, B., Yoshida, M. and Horinouchi, S. (1999). Leptomycin B inactivates CRM1/exportin 1 by covalent modification at a cysteine residue in the central conserved region. *Proc. Natl. Acad. Sci. USA* **96**, 9112-9117.
Kumar, A., Eby, M. T., Sinha, S., Jasmin, A. and Chaudhary, P. M. (2001). The ectodermal dysplasia receptor activates the nuclear factor-κB, JNK, and cell death pathways and binds to ectodysplasin A. *J. Biol. Chem.* **276**, 2668-2677.
Lamkanfi, M., D'hondt, K., Vande Walle, L., van Gurp, M., Denecker, G., Demeulemeester, J., Kalai, M., Declercq, W., Saelens, X. and Vandenabeele, P. (2005). A novel caspase-2 complex containing TRAF2 and RIP1. *J. Biol. Chem.* **280**, 6923-6932.
Lamkanfi, M., Festjens, N., Declercq, W., Vanden Berghe, T. and Vandenabeele, P. (2007). Caspases in cell survival, proliferation and differentiation. *Cell Death. Differ.* **14**, 44-55.
Lange, R. W., Germolec, D. R., Foley, J. F. and Luster, M. I. (1998). Antioxidants attenuate anthralin-induced skin inflammation in BALB/c mice: role of specific proinflammatory cytokines. *J. Leukoc. Biol.* **64**, 170-176.
Lawrence, T. (2009). The nuclear factor NF-kappaB pathway in inflammation. *Cold Spring. Harb. Perspect. Biol.* **1**, a001651.
Lawrence, T. and Fong, C. (2010). The resolution of inflammation: anti-inflammatory roles for NF-κB. *Int. J. Biochem. Cell Biol.* **42**, 519-523.
Laychock, S. G., Sessanna, S. M., Lin, M.-H. and Mastrandrea, L. D. (2006). Sphingosine 1-phosphate affects cytokine-induced apoptosis in rat pancreatic islet beta-cells. *Endocrinology* **147**, 4705-4712.
Li, Q. and Verma, I. M. (2002). NF-kappaB regulation in the immune system. *Nat. Rev. Immunol.* **2**, 725-734.
Marchetti, S., Gamas, P., Belhacène, N., Grosso, S., Pradelli, L. A., Colosetti, P., Johansen, C., Iversen, L., Deckert, M., Luciano, F. et al. (2009). The caspase-cleaved form of LYN mediates a psoriasis-like inflammatory syndrome in mice. *EMBO J.* **28**, 2449-2460.
May, M. J. and Ghosh, S. (1998). Signal transduction through NF-kappa B. *Immunol. Today* **19**, 80-88.
Nemergut, M. E., Lindsay, M. E., Brownawell, A. M. and Macara, I. G. (2002). Ran-binding protein 3 links Crm1 to the Ran guanine nucleotide exchange factor. *J. Biol. Chem.* **277**, 17385-17388.
Newton, K. and Dixit, V. M. (2012). Signaling in innate immunity and inflammation. *Cold Spring. Harb. Perspect. Biol.* **4**, a006049.
Oeckinghaus, A. and Ghosh, S. (2009). The NF-κB family of transcription factors and its regulation. *Cold Spring. Harb. Perspect. Biol.* **1**, a000034.
Oeckinghaus, A., Hayden, M. S. and Ghosh, S. (2011). Crosstalk in NF-kappaB signaling pathways. *Nat. Immunol.* **12**, 695-708.
Ozes, O. N., Mayo, L. D., Gustin, J. A., Pfeffer, S. R., Pfeffer, L. M. and Donner, D. B. (1999). NF-kappaB activation by tumour necrosis factor requires the Akt serine-threonine kinase. *Nature* **401**, 82-85.
Pasparakis, M. (2009). Regulation of tissue homeostasis by NF-κB signalling: implications for inflammatory diseases. *Nat. Rev. Immunol.* **9**, 778-788.
Pasparakis, M., Courtois, G., Hafner, M., Schmidt-Supprian, M., Nenci, A., Toksoy, A., Krampert, M., Goebeler, M., Gillitzer, R., Israel, A. et al. (2002). TNF-mediated inflammatory skin disease in mice with epidermis-specific deletion of IKK2. *Nature* **417**, 861-866.
Perkins, N. D. (2007). Integrating cell-signalling pathways with NF-κB and IKK function. *Nat. Rev. Mol. Cell Biol.* **8**, 49-62.
Romashkova, J. A. and Makarov, S. S. (1999). NF-κB is a target of AKT in anti-apoptotic PDGF signalling. *Nature* **401**, 86-90.
Salmena, L., Lemmers, B., Hakem, A., Matysiak-Zablocki, E., Murakami, K., Au, P. Y. B., Berry, D. M., Tamblyn, L., Shehabeldin, A., Migon, E. et al. (2003). Essential role for caspase 8 in T-cell homeostasis and T-cell-mediated immunity. *Genes. Dev.* **17**, 883-895.
Schmidt, K. N., Podda, M., Packer, L. and Baeuerle, P. A. (1996). Anti-psoriatic drug anthralin activates transcription factor NF-kappa B in murine keratinocytes. *J. Immunol.* **156**, 4514-4519.
Sen, R. and Baltimore, D. (1986a). Inducibility of kappa immunoglobulin enhancer-binding protein Nf-kappa B by a posttranslational mechanism. *Cell* **47**, 921-928.
Sen, R. and Baltimore, D. (1986b). Multiple nuclear factors interact with the immunoglobulin enhancer sequences. *Cell* **46**, 705-716.
Stoven, S., Silverman, N., Junell, A., Hedengren-Olcott, M., Erturk, D., Engstrom, Y., Maniatis, T. and Hultmark, D. (2003). Caspase-mediated processing of the *Drosophila* NF-κB factor Relish. *Proc. Natl. Acad. Sci. USA* **100**, 5991-5996.
Stratis, A., Pasparakis, M., Markur, D., Knaup, R., Pofahl, R., Metzger, D., Chambon, P., Krieg, T. and Haase, I. (2006). Localized inflammatory skin disease following inducible ablation of I kappa B kinase 2 in murine epidermis. *J. Invest. Dermatol.* **126**, 614-620.
Su, H., Bidere, N., Zheng, L., Cubre, A., Sakai, K., Dale, J., Salmena, L., Hakem, R., Straus, S. and Lenardo, M. (2005). Requirement for caspase-8 in NF-κB activation by antigen receptor. *Science* **307**, 1465-1468.
Trahey, M. and McCormick, F. (1987). A cytoplasmic protein stimulates normal N-ras p21 GTPase, but does not affect oncogenic mutants. *Science* **238**, 542-545.
Vallabhapurapu, S. and Karin, M. (2009). Regulation and function of NF-κB transcription factors in the immune system. *Annu. Rev. Immunol.* **27**, 693-733.
Verma, I. M., Stevenson, J. K., Schwarz, E. M., Van, A. D. and Miyamoto, S. (1995). Rel/NF-kappa B/I kappa B family: intimate tales of association and dissociation. *Genes Dev.* **9**, 2723-2735.
Viatour, P., Merville, M.-P., Bours, V. and Chariot, A. (2005). Phosphorylation of NF-κB and IκB proteins: implications in cancer and inflammation. *Trends Biochem. Sci.* **30**, 43-52.
Wambier, C. G., Ramalho, L. N., Frade, M. A. and Foss, N. T. (2014). NFκB activation in cutaneous lesions of leprosy is associated with development of multibacillary infection. *J. Inflamm. Res.* **7**, 133-138.
Weissgerber, T. L., Milic, N. M., Winham, S. J. and Garovic, V. D. (2015). Beyond bar and line graphs: time for a new data presentation paradigm. *PLoS. Biol.* **13**, e1002128.
Wen, L.-P., Madani, K., Martin, G. A. and Rosen, G. D. (1998). Proteolytic cleavage of Ras GTPase-activating protein during apoptosis. *Cell Death Differ.* **5**, 729-734.
Widmann, C., Gibson, S. and Johnson, G. L. (1998). Caspase-dependent cleavage of signaling proteins during apoptosis. A turn-off mechanism for anti-apoptotic signals. *J. Biol. Chem.* **273**, 7141-7147.
Wong, E. T. and Tergaonkar, V. (2009). Roles of NF-κB in health and disease: mechanisms and therapeutic potential. *Clin. Sci.* **116**, 451-465.
Yamamoto, Y. and Gaynor, R. B. (2001). Therapeutic potential of inhibition of the NF-κB pathway in the treatment of inflammation and cancer. *J. Clin. Invest.* **107**, 135-142.
Yang, J.-Y. and Widmann, C. (2001). Antiapoptotic signaling generated by caspase-induced cleavage of RasGAP. *Mol. Cell. Biol.* **21**, 5346-5358.
Yang, J.-Y. and Widmann, C. (2002). The RasGAP N-terminal fragment generated by caspase cleavage protects cells in a Ras/PI3K/Akt-dependent manner that does not rely on NFκB activation. *J. Biol. Chem.* **277**, 14641-14646.
Yang, J.-P., Hori, M., Sanda, T. and Okamoto, T. (1999). Identification of a novel inhibitor of nuclear factor-κB, RelA-associated inhibitor. *J. Biol. Chem.* **274**, 15662-15670.
Yang, J.-Y., Michod, D., Walicki, J., Murphy, B. M., Kasibhatla, S., Martin, S. J. and Widmann, C. (2004). Partial cleavage of RasGAP by caspases is required for cell survival in mild stress conditions. *Mol. Cell. Biol.* **24**, 10425-10436.
Yang, J.-Y., Walicki, J., Abderrahmani, A., Cornu, M., Waeber, G., Thorens, B. and Widmann, C. (2005a). Expression of an uncleavable N-terminal RasGAP fragment in insulin-secreting cells increases their resistance toward apoptotic stimuli without affecting their glucose-induced insulin secretion. *J. Biol. Chem.* **280**, 32835-32842.
Yang, J.-Y., Walicki, J., Michod, D., Dubuis, G. and Widmann, C. (2005b). Impaired Akt activity down-modulation, caspase-3 activation, and apoptosis in cells expressing a caspase-resistant mutant of RasGAP at position 157. *Mol. Biol. Cell* **16**, 3511-3520.
Yoon, S.-O., Shin, S., Liu, Y., Ballif, B. A., Woo, M. S., Gygi, S. P. and Blenis, J. (2008). Ran-binding protein 3 phosphorylation links the Ras and PI3-kinase pathways to nucleocytoplasmic transport. *Mol. Cell* **29**, 362-375.